

# Communication Subsystems for Emerging Wireless Technologies

Zbynek RAIDA, Zdenek KOLKA, Roman MARSALEK, Jiri PETRZELA, Ales PROKES,  
Jiri SEBESTA, Tomas GOTTHANS, Zdenek HRUBOS, Zdenek KINCL, Lukas KLOZAR,  
Ales POVALAC, Roman SOTNER, Petr KADLEC

Dept. of Radio Electronics, Brno University of Technology, Purkynova 118, 612 00 Brno, Czech Republic

raida@feec.vutbr.cz

**Abstract.** *The paper describes a multi-disciplinary design of modern communication systems. The design starts with the analysis of a system in order to define requirements on its individual components. The design exploits proper models of communication channels to adapt the systems to expected transmission conditions. Input filtering of signals both in the frequency domain and in the spatial domain is ensured by a properly designed antenna. Further signal processing (amplification and further filtering) is done by electronic circuits. Finally, signal processing techniques are applied to yield information about current properties of the frequency spectrum and to distribute the transmission over free subcarrier channels.*

## Keywords

Communication system, long term evolution (LTE), WiMAX, radio frequency identification (RFID), cognitive radio, Nyquist  $\delta$ -filter, channel modeling, antenna system, Yagi-Uda antenna, multi-objective optimization, Multi-Objective Self-Organizing Migrating Algorithm (MOSOMA), amplifier, tunable oscillator, circuit analysis, circuit testing, dirty RF signal processing, multicarrier system optimization, spectrum sensing.

## 1. Introduction

Development of novel communication systems tends to provide high speed and high reliability services. Requirements on both speed and reliability require a sufficiently wide band of operation frequencies. In order to solve the problem, communication services can be shifted to higher frequency bands or spectrum-efficient techniques have to be applied.

In the case of higher frequency bands, a tremendous development can be observed at frequencies around 60 GHz [1.1] and in frequency bands 71 to 76 GHz, 81 to 86 GHz and 92 to 95 GHz [1.2], [1.3].

In the case of spectrum-efficient techniques, intensive research is focused on cognitive systems. A cognitive system scans an electromagnetic environment, analyses the frequency spectrum, and identifies free frequency sub-bands. Identified sub-bands are consecutively used for communication by a multi-carrier system [1.4] to [1.6].

In Europe, the research of emerging communication techniques comprising both higher frequency bands and spectrum efficient techniques is coordinated by the COST Action IC0803 *RF/Microwave Communication Subsystems for Emerging Wireless Technologies*. The Czech Republic is represented by the Czech Technical University in Prague and Brno University of Technology in this COST Action. The research of emerging communication techniques is supported by the Czech Ministry of Education by the grants OC09016 Components and Advanced Radio Communication Systems and OC09075 Emerging Wireless Systems.

In this paper, we summarize research performed by Brno University Technology in the frame of the COST Action IC0803 and the grant project OC09016.

We conceived our research as an interdisciplinary one and a complex one because the design of separate components of sophisticated communication systems has to consider the functionality of the system in its whole. When designing a communication component, requirements on the system have to be considered in its whole, and specific features of other components in the system have to be taken into account.

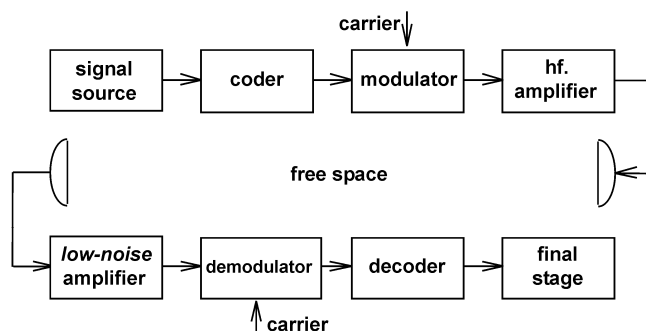


Fig. 1.1. Block diagram of a radio communication system.

Fig. 1.1 shows a general block diagram of a radio communication system. Examples of specific systems, which are intensively investigated these days, are briefly reviewed in Section 2.

During the design, specific properties of propagation of electromagnetic waves in a given frequency band and a given environment (free space, urban area, interiors of buildings, etc.) have to be considered. Propagation of electromagnetic waves is discussed in Section 3.

In order to transform the electromagnetic wave propagating in free space to signals propagating inside the receiving system and vice versa, proper antennas have to be synthesized. Section 4 deals with antenna research.

In Section 5, development of advanced circuitry for communication systems is discussed. Attention is turned to electronic control of circuitry, to the design of oscillators with precise smooth adjustment of frequency, and to the methods of circuit analysis and testing.

Signal processing issues are discussed in Section 6. Attention is turned to so-called dirty-RF signal processing to achieve a maximal power efficiency of communication systems with minimized distortions. The maximal spectrum efficiency is going to be achieved by the exploitation of spectrum sensing and optimization of multi-carrier systems. Section 7 concludes the paper.

## 2. Radio Communication Systems

In general, recent trends in research of radio communication systems can be divided into two fundamental strategies. Both ways are closely related to the limited frequency bands and to the requirements for increasing the amount of transferred information.

The first strategy is aimed at exploiting higher operating frequencies above 10 GHz. The second direction is focused on the effective utilization of channel capacity by using new modulation and coding techniques, diversity systems, precise channel modeling and communication scheme adaptations, and availing of temporary unoccupied bands.

These approaches include adaptive modulations, iterative decoding, multiple-input multiple output (MIMO) systems, and cognitive radio. All these methods are aimed at efficient usage of the frequency spectrum. Obviously, the successful application of these methods has to be supported by new structures such as inter-symbol interference symbol filters. On the other hand, these new approaches offer new bonus features such as precise positioning of communicating devices. Chosen aspects of this area are discussed in the following paragraphs.

### 2.1 Cognitive Radio

The cognitive radio (CR) is a promising but also controversial approach to the effective exploitation of the

radio spectrum. According to [2.1], the CR can be defined as an intelligent wireless communication system which is aware of its environment and uses learning methods to achieve high reliability and efficient spectrum utilization.

The dynamic spectrum access is the key component of the CR. The dynamic spectrum access is used to overcome the problem with limited available spectrum resources. The free spectrum can be detected using two different approaches; spectrum sensing (see Section 6) and geo-location. Both these approaches have found their place during the standardization process of the first two standards based on the CR principle, the WRAN standard IEEE 802.22 [2.2] and the new WiFi in TV White-Spaces standard IEEE 802.11af.

During recent years, we have performed a measurement campaign in order to show the potential for the dynamic spectrum access. We performed research in cooperation with ESIEE Paris (France). Measurement results from geographical regions of Brno and Paris have been presented in [2.3].

### 2.2 Nyquist $\delta$ Filters

Almost all digital radio transceivers, which process an incoming data signal on the sample-by-sample basis, use matched pulse shaping filters with their cascade satisfying the Nyquist condition for the minimum inter-symbol interference (ISI). Most of them have to simultaneously fulfill strict limits of adjacent and alternate channel power attenuation or respect other requirements such as maximizing robustness against timing jitter [2.4], [2.5], [2.6], minimizing the duration of the impulse response [2.7], [2.8] or minimizing the peak-to-average power ratio (PAPR) at the transmitter filter output [2.9].

The most widely used Nyquist filter is of the raised cosine (RC) type [2.4]. It is usually split into two transmitter and receiver parts in order to fulfill the matched filtering condition for maximizing the signal-to-noise ratio at the decision stage.

Frequency response of many other published generalized Nyquist filters can be regarded as a convolution of the response of a RC filter and a shaping window which exhibits different convergence than zero. Typical weighting windows of this type are the Hann window or generally defined as the Blackman window, which can be continuously changed to the Blackman, exact-Blackman, Blackman-Harris and  $\cos^4(x)$  [2.10]. The design of the digital filter thus consists in selecting an appropriate window function which exhibits the specific behavior of the resulting filter in the time or frequency domain. There is also a set of Nyquist filters which are based on a different function than the RC filter. One of them, the modulation filter, is defined as a *better* than the Nyquist filter (BN filter) [2.11].

The recent research in this area is aimed [2.12] at developing a set of Nyquist filters which could exhibit:

- Reasonably balanced time and frequency-domain parameters with respect to a minimum residual inter-symbol interference filter;
- Satisfactory stop-band attenuation, which is directly related to an adjacent channel power as one of the most critical parameters of several practical applications.

The presented work proposes a general Nyquist  $\delta$ -filter (ND filter) based on a decomposed Blackman weighting window. The ND filter is defined in the frequency domain as

$$G_{\delta}(f) = \begin{cases} 1, & 0 \leq f \leq B(1 - \alpha_0 - \delta) \\ 1 - \cos[f(\alpha_0, \delta)]^4, & B(1 - \alpha_0 - \delta) < f \leq B \\ \cos[f(\alpha_0, \delta)]^4, & B < f \leq B(1 + \alpha_0 + \delta) \\ 0 & B(1 + \alpha_0 + \delta) \leq f \end{cases} \quad (2.1)$$

where

$$f(\alpha_0, \delta) = \frac{\pi[B(1 + \alpha_0) - (f + \delta)]}{4B\alpha_0},$$

$$\delta = 0.5 - B(1 - \alpha_0) - \frac{4B\alpha_0}{\pi} \arccos\left(\frac{1}{2^{1/4}}\right).$$

$B$  is the single-sided filter bandwidth corresponding to the Nyquist frequency  $1/2T_s$  ( $T_s$  is the symbol period). In order to get the Nyquist  $\delta$ -filter definition directly comparable to the typical RC filter notation, the roll-off factor  $\alpha_{RC}$  can be expressed as  $\alpha_{RC} = \alpha_0 + \delta$ . When comparing both filters, the RC filter will have an equivalent excess bandwidth adjusted by the value of the  $\delta$  parameter. Digital filter coefficients can be calculated from (2.1) by the inverse Fourier transform of the frequency response

$$g_{\delta}(t) = \frac{\pi}{2} \int_{-B(1+\alpha)}^{B(1+\alpha)} G_{\delta} e^{2\pi ft} df \quad (2.2)$$

and by the equidistant sampling of the continuous impulse response (2.2) over the limited time interval, which is defined by the group delay parameter  $G_D$ .

In order to compare the substantial property of different Nyquist filters, specific evaluation criteria such as the relative level of the residual ISI, the level of impulse response side lobes or the stop-band attenuation, were defined and numerically calculated [2.12]. The comparison of the amplitude frequency characteristics of the truncated RC filter, the BN filter and the proposed ND filter is shown in Fig. 2.1. Comparison of the normalized impulse responses of these filters is given in Fig. 2.2.

The Nyquist  $\delta$ -filter set enlarges the family of Nyquist filters. When compared with the truncated square root raised cosine filter cascade, the Nyquist  $\delta$ -filter improves frequency domain parameters while reaching a low level of the residual inter-symbol interference. The improvement is reached at the cost of a higher side lobe level of the impulse response.

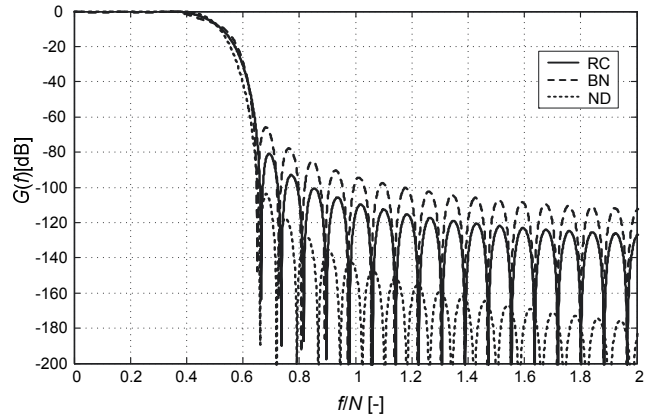


Fig. 2.1. Amplitude frequency characteristics of the RC filter (RC); better than Nyquist filter (BN); Nyquist  $\delta$ -filter (ND) of the same filter order and equivalent excess bandwidth  $\alpha=0.284$ ;  $N=5$ ;  $G_D=2 \times 6$ .

An exact symbolic definition of the Nyquist  $\delta$ -filter in the frequency domain gives the designer the scope to choose freely the filter parameters such as the equivalent excess bandwidth, the group delay and over-sampling parameters. Moreover, the symbolic definition enables to derive coefficients for either the *normal* or the square root filter variants. The presented filters generated are of linear-phase having symmetrical impulse responses, which directly contribute to efficient hardware realization structures.

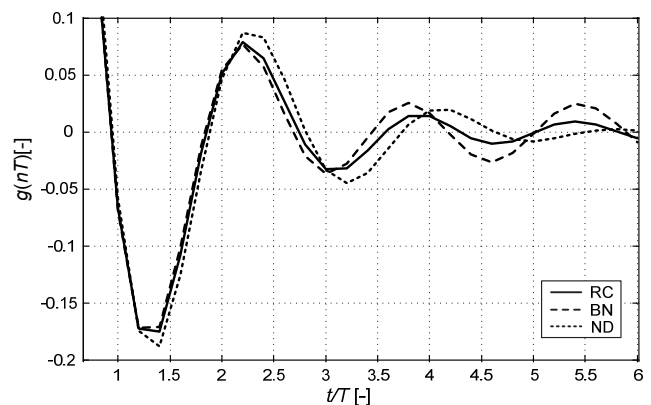


Fig. 2.2. Normalized impulse responses of the RC filter (RC); better than Nyquist filter (BN); Nyquist  $\delta$ -filter (ND).  $\alpha=0.284$ ;  $N=5$ ;  $G_D=2 \times 6$ .

### 2.3 RFID Tag Positioning

In recent years, radio-frequency identification (RFID) has moved to mainstream applications. RFID uses radio communication to identify a physical object.

This Section provides an introduction to the principles of RFID spatial identification. Long range positioning and localization is a common topic, widely discussed also in the areas of radar systems and wireless networks [2.13]. On the contrary, short range distance estimation is very specific to RFID backscattering principles, and the research in this area has started in recent years.

The most common method of distance estimation is based on the received signal strength (RSS) of RFID signals. The measurement is implemented in majority of commercial RFID readers, but many drawbacks can be identified here. The signal power at a reader with a round-trip loss strongly depends on the environment where the RFID system is deployed.

The signal power at a reader can be expressed as

$$P_{RX} = P_{TX} \cdot \eta \cdot G_{tag}^2 G_{reader}^2 \cdot \left( \frac{\lambda}{4\pi d} \right)^{2n} \quad (2.3)$$

where  $P_{TX}$  is the power transmitted by the reader,  $\eta$  is the power transfer efficiency of the tag,  $G_{tag}$  and  $G_{reader}$  are the antenna gain of the tag and the reader, respectively,  $\lambda$  is the wavelength,  $d$  is the range between the tag and the reader, and  $n$  is the path loss exponent. The typical value of  $\eta$  is  $-5$  dB and depends on the power received by the tag among others. The path loss exponent  $n$  is defined by the environment and varies between 1.6 for indoor line of sight and 6.0 for outdoor propagation. As a result, the range estimation based on RSS is very inaccurate in general. For reasonable precision, we have to characterize the environment, compensate the nonlinear coefficient of the tag  $\eta$ , and specify antenna orientation with  $G_{tag}$  correction.

The second approach to distance estimation is based on the measurement of round-trip propagation time of flight (ToF). Its application in conventional narrowband RFID systems is difficult because of the poor time resolution limited by the frequency bandwidth. Nevertheless, these techniques are promising for ultra-wideband (UWB) RFID systems, where the sufficient signal bandwidth is available.

The third method employs the phase-of-arrival (PoA) measurement. Two transmitted continuous-wave (CW) signals on different frequencies propagate over the same distance, but their phase delays are proportional to their respective carrier frequencies. This concept is similar to the principle of the dual-frequency radar systems for range estimation. Phase-based techniques of RFID ranging allow coherent signal processing and achieve better performance than the traditional RSS approach [2.14]. On the other hand, a simple PoA measurement fights with phase wrapping. The distance estimation is based on the phase difference observed at two frequencies

$$\hat{d} = \frac{c \cdot \Delta\phi}{4\pi(f_2 - f_1)} + \frac{cm}{2(f_2 - f_1)} \quad (2.4)$$

where  $\Delta\phi$  is the measured phase difference ( $0 \leq \Delta\phi < 2\pi$ ) and  $m$  is an unknown integer. The second term in (2.4) denotes the range ambiguity due to phase wrapping. The maximum unambiguous range is

$$d_{max} = \frac{c}{2(f_2 - f_1)} \quad (2.5)$$

A larger frequency separation is more resistant to noise [2.15] but yields a smaller value of  $d_{max}$ . As long as the tag is stationary, the measurement does not require simultaneously transmitted CW signals. Multiple successive measurements can be performed instead.

Applying simple PoA measurements based on (2.4), only a group delay can be measured. Due to multipath propagation, the distance estimation based on an average of several group delays typically leads to high standard deviations compared to UWB methods.

In [2.16], an overview of phase based ranging techniques has been presented focusing on the phase difference of arrival method measured in the frequency domain (FD-PDoA). After a theoretical overview of the distance estimation and localization techniques, we introduce an experimental RFID front-end prototype used for FD-PDoA measurements. The proposed modular design is very flexible and allows an easy replacement of any block, as well as direct access to all required low-level signals. The main part of this paper is devoted to the range estimation experiments in an anechoic chamber. Several measurement problems are addressed, such as the demodulator phase imbalance correction, the wrapped phase recovery, etc. The ranging is performed with common passive EPC Gen2 RFID tags.

### 3. Propagation of Electromagnetic Waves

Modern communication systems are developing to achieve a higher spectral efficiency, which almost reaches the maximum channel capacity. Multi-diversity systems bring new opportunities for high-performance transmissions. In order to achieve a high data throughput, appropriate channel estimation has to be performed.

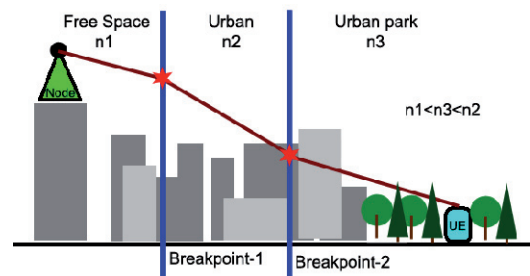


Fig. 3.1. Multi-slope adaptation to a heterogeneous environment. The path loss exponent  $n$  changes the slope of signal level prediction.

The path loss distribution in the channel could be described as time and frequency fading (the Ricean fading for the dominant line-of-sight case, the Rayleigh fading for the non-line-of-sight case) [3.1]. The character of fading depends on the environment (the dominant propagation mechanism), mobility, signal frequency, propagation distance, etc. [3.1].

### 3.1 Radio Propagation Models

Models of radio propagation channels were derived jointly from analytical and empirical methods. Path losses  $PL(d)$  can be described by the log-distance model [3.1]

$$PL(d)|_{dB} = PL_{FS}(d_0) + 10n \log\left(\frac{d}{d_0}\right) + X_\sigma + K_p \quad (3.1)$$

where  $PL_{FS}(d_0) = 2 \cdot 10 \log(\lambda/4\pi d_0)$  is a frequency-dependent parameter describing the free-space path loss at the reference distance  $d_0 = 1$  m [3.1],  $\lambda$  [m] is the wavelength of a signal, and  $d$  [m] is the propagation distance. Next,  $n$  is the path-loss exponent,  $X_\sigma$  [dB] expresses the value of the probability density function with the standard deviation  $\sigma$  [dB]. Finally,  $K_p$  [dB] is an additional correction factor describing individual propagation conditions (height of antennas, rooftops, etc.). The value of the path-loss exponent  $n$  adjusts the slope of the model to correspond with the attenuation character of the environment ( $n = 2$  for the free space propagation). Empirical values for typical propagation scenarios [3.1] are given in Tab. 3.1.

A)		B)	
Environment	Path-loss exponent $n$	Path section	Path loss exponent $n$
Free Space	2.0	Tx-bp0	2.0
Urban	2.7 to 3.5	bp0-bp1	4.5
Urban / shadowed	3.0 to 5.0	bp1-bp2	1.3
Indoor / line of sight	1.6 to 1.8	bp2-bp3	8.6
Indoor / obstructed	4.0 to 6.0	bp3-Rx	2.0

**Tab. 3.1.A)** Values of the path loss exponent  $n$  for various environments [3.1]. **B)** The measured exponent  $n$  for separated sections of the propagation path (Fig. 3.2). Tx is the transmitter, Rx is the receiver, bp0, bp1, bp2, and bp3 are the breakpoints with the values according to Fig. 3.2.

### 3.2 Multi-slope Channel Optimization

The multi-slope approach divides the propagation channel to adjacent sections (Fig. 3.1). The parameters  $n$  and  $X_\sigma$ , in the separated parts are in (3.1) adjusted in compliance with properties of the propagation channel. For example, urban macro cell base stations are typically placed above roof tops of surrounding buildings, and therefore we assume almost free-space conditions for the near side of the propagation path.

In order to adjust the breakpoint positions in the multi-slope model, we applied particle swarm optimization (PSO). The breakpoint positions are indicated by blue and red triangles in Fig. 3.2.

The first break point bp0 is fixed at the distance determined as the free space attenuation. This distance represents the correction of the node height for a macro cell in an urban area.

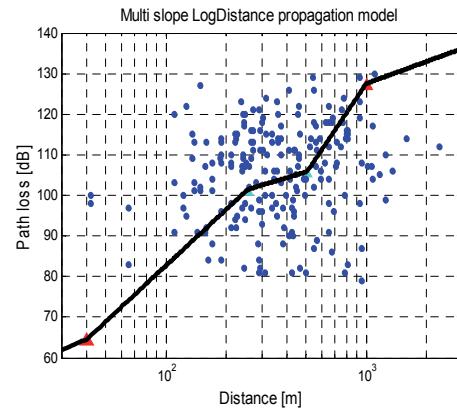


**Fig. 3.2.** Optimized multi-slope log-distance model with a deviation error 12 dB. Breakpoint positions are bp0 = [40 m; 64 dB], bp1 = [253 m; 100 dB], bp2 = [542 m; 104 dB], and bp3 = [1000 m; 127 dB].

The PSO algorithm estimated the position of the breakpoints (bp1, bp2, bp3) in the range from 40 m to 1000 m. The algorithm changes the position (the distance and the level) of the breakpoints and model path losses according to (3.1). The obtained path loss exponents for separate sections are summarized in Tab. 3.1. Outdoor channel modeling and measurement were presented in [3.2].

The multi-slope optimization algorithm was applied for the indoor path-loss modeling. Here, the multipath propagation is the dominant propagation mechanism. The line of sight can be applied for the propagation within a single room only. Materials and the inner structure of the interior affect the fading effect ( $X_\sigma$ ). Walls and floors determine the breakpoint positions. Simulation of the propagation in an indoor environment for 2.5 GHz band was published in [3.3].

A valid description of a propagation channel requires adaptive channel estimation based on a continuous measurement in the area of interest.

## 4. Antenna Synthesis

Considering cognitive systems, special requirements are formulated for antennas. Frequency response of the antenna gain in the defined direction should exhibit filtering properties. In the operating band of the antenna, the gain is expected to be constant and relatively high. Out of the operating band, the gain is required to be very small. Thanks to this property, sub-channels for the transmission can be freely allocated in the operating band, and signals with frequencies out of the operating band are strongly suppressed by the antenna. There are two ways to reach the described behavior of the antenna:

- Shaping the directivity pattern of the antenna. Elements of an antenna structure are associated by amplitudes and phases of currents, which can focus

the main beam of the antenna to the direction of communication in the operating band, and to the opposite direction out of the operating band. That way, we swap in between a high gain and a low gain in the direction of communication.

- Synthesizing impedance characteristics of the antenna. We try to complete the antenna by an additional filtering structure, which is an inherent part of the antenna geometry (the structure is called *filtenna*). The additional filtering structure ensures a bad impedance matching of the filtenna out of the operating band and a good matching in the operating band. That way, a very small value of the gain is obtained out of the operating band and vice versa.

From the viewpoint of the transmitted power out of the operating band, the first approach gives the power off into the direction, where no communication is expected, and the second approach reflects the power back to the source by a strong impedance mismatch at the antenna input.

In the following paragraph, we exploit global multi-objective optimization for shaping the radiation pattern of a Yagi antenna. Thus, we follow the first approach to the synthesis of the frequency response of the gain.

### 4.1 Yagi-Uda Antenna Optimization

The concept of the Yagi-Uda antenna provides a sufficient number of degrees of freedom for a designer. Therefore, several authors have been concerned with the optimal design of Yagi-Uda antennas, [4.1] to [4.3]. As described in [4.1], the gain of the Yagi-Uda antenna is a highly non-linear function of antenna element lengths and spacing between elements.

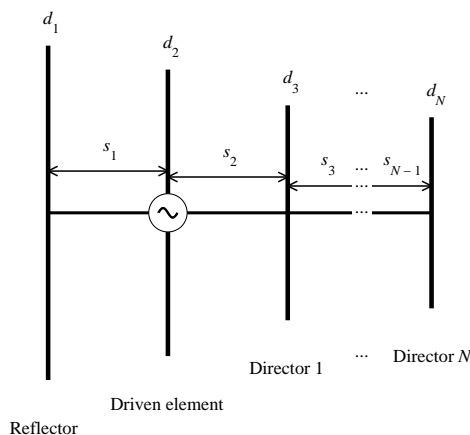


Fig. 4.1. Description of an  $N$ -element Yagi-Uda antenna.

The model of the Yagi-Uda antenna is depicted in Fig. 4.1. Here,  $d_n$  denotes the length of the  $n$ -th element and  $s_n$  stands for the distance between the  $n$ -th element and the  $(n + 1)$  one. The first element serves as a reflector, the second element is the only fed element, and the rest of the elements serve as directors for the outgoing wave. Considering an antenna with  $N$  elements,  $(2N - 1)$  parameters

can be changed to achieve a required frequency response of the gain.

Almost every design problem takes into consideration more than one objective. Usually, these objectives are conflicting, and therefore, just a single optimal solution fulfilling all the requirements at the same time cannot be found [4.4]. Then, the solution of the multi-objective problem is a so-called Pareto front, which expresses a trade-off between all objectives.

We have derived a novel optimizer to deal with multi-objective problems in [4.5]. The method is called the Multi-Objective Self-Organizing Migrating Algorithm (MOSOMA). The agents (vectors of optimized parameters) migrate through the decision space (space of optimized parameters). Objective functions are evaluated in every visited position, and their values are shared by the whole group of agents. Information from the objective space controls the migration procedure and leads all agents closer to the Pareto front region. MOSOMA is able to deal with both unconstrained and constrained problems having any number of objectives and continuous or discrete optimized parameters [4.6].

Special requirements on the properties of the antenna lead to the formulation of the following two-objective constrained problem:

$$F_1 = -\frac{1}{P} \sum_{p=1}^P G(f_p, \theta_0), \tag{4.1}$$

$$F_2 = \frac{1}{S} \sum_{s=1}^S G(f_s, \theta_0).$$

Here,  $P$  and  $S$  denote the number of frequency points in the pass band and stop band of the antenna,  $G$  stands for the gain,  $f_p$  and  $f_s$  are pass band and stop band frequencies and  $\theta_0$  stands for the desired angle of radiation. The first objective maximizes the gain in the pass-band while the second one minimizes it in the stopping band. The impedance matching of the antenna is controlled by the following constraint:

$$\begin{aligned} |50 - \text{Re}(Z_{in})| < 5, \\ |\text{Im}(Z_{in})| < 10. \end{aligned} \tag{4.2}$$

Here,  $Z_{in}$  stands for the input impedance of the Yagi-Uda antenna. The length of the elements can change in the interval  $0.3\lambda < d_n < 0.7\lambda$  and spacing between neighboring elements in the interval  $0.2\lambda < d_n < 0.6\lambda$  for purposes of the optimization.

The Pareto front found by MOSOMA (the best front achieved from ten runs of MOSOMA, 25 000 objective-function computations) is depicted in Fig. 4.3. Three interesting points are highlighted in the picture: the best solutions according to the  $F_1$  and  $F_2$  objectives and the trade-off solution. The frequency dependence of the gain is depicted in Fig. 4.3 for these three solutions. The pass band  $f_p$  and the stop band  $f_s$  are marked here by dashed lines. Only the trade-off solution fulfills both the objectives satisfactorily.

Parameters of those designs are summarized in Tab. 4.1. All the designs satisfy requirements defined by the constraint function (4.2). The standing wave ratio is  $VSWR = 1.09$  for the trade-off design.

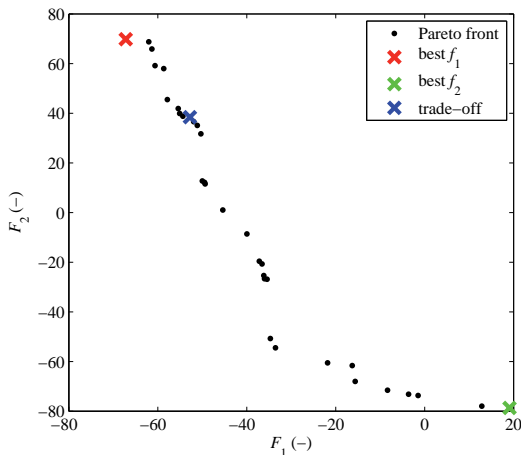


Fig. 4.2. Pareto front found by MOSOMA.

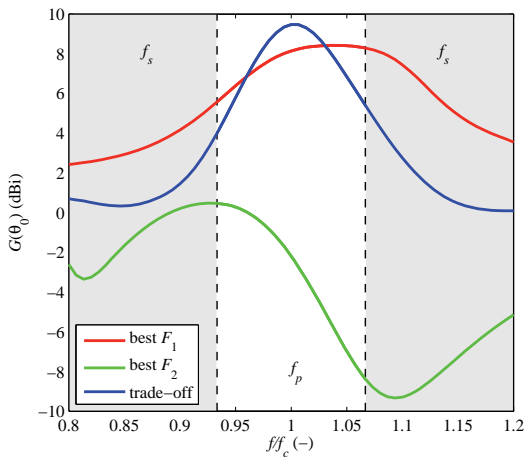


Fig. 4.3. Frequency dependence of gain.

n	best $F_1$		best $F_2$		trade-off	
	$d(\lambda)$	$s(\lambda)$	$d(\lambda)$	$s(\lambda)$	$d(\lambda)$	$s(\lambda)$
1	0.667	0.493	0.457	0.293	0.482	0.220
2	0.455	0.242	0.443	0.354	0.436	0.425
3	0.451	0.341	0.351	0.441	0.434	0.466
4	0.580	0.348	0.324	0.369	0.390	0.381
5	0.582	0.574	0.300	0.483	0.354	0.409
6	0.668	0.486	0.418	0.233	0.620	0.294
7	0.597	-	0.368	-	0.432	-
$Z_{in}(\Omega)$	49.87 - 1.97i		54.09 - 6.86i		48.04 + 3.57i	
VSWR (-)	1.04		1.17		1.09	

Tab. 4.1. Parameters of the designs found by MOSOMA.

## 5. Advanced Circuits

Recent communication systems tend to operate with high data rates. We have to therefore design analog subsystems which are capable of generating or handling high-

frequency signals. Speaking in terms of analog signal processing, we are particularly focused on oscillators, filters and mixers.

It turns out that the utilization of current-mode active building blocks is a good choice for high-frequency applications. Moreover, there are a number of such devices with transfer parameters which are externally controllable by a DC source.

The list of advanced active devices is given in [5.1]. Among well-known off-the-shelf elements (multiple-output transconductance amplifiers MOTA, current-conveyor CC, CC with differential input voltage DVCC, etc.) also more complex hypothetical blocks are provided, some of them comprising useful mathematical operations. Even though these devices are not commercially available, they can still be implemented by using a suitable connection of controlled sources.

Due to the communication system miniaturization, we are looking for network structures, which are ready for the on-chip implementation. Thus, research and experimentation in this field can uncover new circuits with promising properties like a good behavior match with a mathematical model, a low supply voltage leading to the decreased power consumption, universality, minimum number of external passive elements, a small necessary chip area, etc.

### 5.1 Electronic Control in Filter Structures

In the case of biquad filters, an independent electronic adjustment of the quality factor and pole frequency is the basic requirement. Many circuit topologies have been already discovered, analyzed, verified and published. For example, the network solution presented in [5.2] contains all types of the second-order transfer functions, and allows wide-range electronic tuning of the pole frequency and bandwidth of the band-pass filter by one parameter only.

Several MOTAs with  $g_m = f(I_{set})$  control were used as active devices in a multi-loop feedback system. It turns out that follow-the-leader structure, similar to this circuit, can be designed so that the electronic control of the transfer function zeroes continuously changes the frequency response from the band-reject filter to the all-pass filter. After further design considerations, we can also develop an externally adjustable filter which effectively combines a modified low-pass response, a band-reject response, and a high-pass frequency response.

A current gain control was used in [5.3] where innovative circuits for modeling active elements as current follower (CF) and current amplifier (CA) with the intrinsic resistance and the gain control were introduced and used in an application of a multi-functional biquad, see Fig. 5.1. Among other employed active blocks, the voltage buffer (VB) and the current feedback amplifier (CFA) can be recognized. High-pass and band-pass outputs are typical for this network configuration.

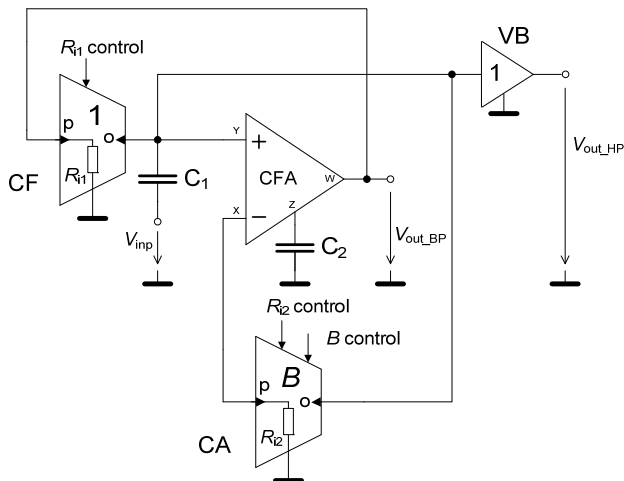


Fig. 5.1. Adjustable biquad with two types of external control.

Filters and oscillators dedicated to arbitrary high-frequency applications require a detailed study of the real circuit behavior. The study should describe a way how parasitic features of active blocks can influence overall theoretical parameters of the circuit. To be more specific, roll-off factors of current gains or transconductances, input and output impedances belong to the main problematic parts.

Additional difficulties should be solved if the output responses are accessible through a grounded passive element only, or if these responses (band-stop ones especially) are mirrored by simple current followers [5.4].

The active elements with low output impedances have an analogical impact on the stop-band attenuation in current-mode circuits. The question on the significant minimization of these influences was answered for one filter structure in [5.5].

In general, the active elements should be treated as nonlinear ones due to the saturation of the output voltage or the current. Moreover, parasitic capacitances can boost the order of the circuit and enrich the global behavior so that the noise-like chaotic motion can be observed [5.6].

## 5.2 Tunable Harmonic Oscillators

The class of analog oscillators with a precise smooth electronic adjustment of a harmonic waveform frequency seems to be a useful core block for modulators, demodulators or signal generators. Very simple networks, where only two active devices (MOTA and electronically controlled CC) were implemented, were introduced in [5.7] and [5.8]. Here, only three or four passive elements are required.

The condition for the system being on the stability boundary (CO), and the associated frequency of the oscillation (FO) are controllable via an external DC source (transconductances and current gain).

Only a single active element (the current gain controlled current conveyor transconductance amplifier, CGC-

CCTA) was used in the quadrature oscillator [5.9]. Advantageously, all four passive elements are grounded. The FO depends on current gain and CO on the grounded resistor.

The improved version of the amplifier was published in [5.10]. Here, CO is also covered by the current gain. However, this network is more complicated than the previous one.

Recently, we also proposed circuit solutions where the current gain control and the voltage gain control are employed simultaneously. Two active elements are sufficient for the operation with the linear FO control while achieving large stable output amplitudes [5.11].

The oscillators are also subject to higher-order dynamical motion like quasi-periodicity and chaos. A gallery of basic second-order systems with the periodic solution and diamond transistors (DT) as active elements is provided in [5.12]. We can demonstrate that lowering the values of working capacitances can lead to the evolution of strange state space attractors.

Even though new information given in the above mentioned papers is not far beyond the current knowledge of linear circuits, it is a good starting point for the complex high-speed system-on-chip integration.

Many results were validated by thorough laboratory measurements with discrete active elements used to implement more complicated building blocks. A circuit model on the transistor-layout-level for each active device was derived using appropriate microelectronic fabrication technology.

## 5.3 Methods for Circuits Analysis and Testing

The circuit design requires adequate tools and methods for analysis, simulation, and testing. Nowadays, a number of numerical simulators ranging from a simple SPICE to an advanced RF Class are available to designers [5.13]. In contrast to the numerical simulation, a single symbolic formula concentrates information about circuit behavior for any combination of parameters of network elements within a certain range.

Research activities within the project were focused on overcoming the main disadvantage of an exact symbolic analysis in the frequency domain, which is the exponential growth of the expression complexity with the circuit size. If we appropriately restrict the range of frequency and network parameters, the majority of symbolic terms can be removed from large expressions without any significant numerical error [5.14].

From a practical point of view, methods which simplify a circuit model are more computationally feasible in comparison with methods simplifying the final expressions [5.15]. The only commercially available symbolic simplification tool *Analog Insydes* implements a matrix-based method [5.16] where individual matrix elements are removed to obtain a simplified solution. In some cases, this

equation simplification may surprisingly add symbolic terms that were not present in the original expression. Another method [5.17] is based on a heuristic approach consisting in modifying the graphs of the numerator and the denominator separately. However, this approach does not have a clear physical interpretation.

We have developed a new method based on physical relations in the circuit. The simplification process is based on removing branches with negligible voltages from high-voltage loops and low-current branches from high-current cuts [5.18], [5.19]. The algorithm mimics what a designer does intuitively during the hand simplification of the circuit analyzed. The process of the automated model simplification is based on numerical comparisons of the simplified responses and the reference responses, usually for nominal values of network elements. The method from [5.19] can be easily extended to take into account parameter variations. An algorithm for the worst-case simplification was published in [5.20].

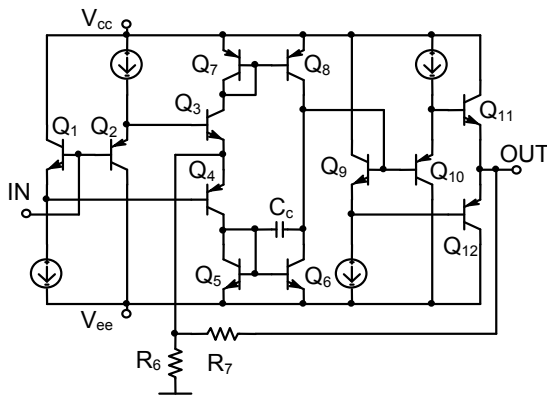


Fig. 5.2. Circuit with current-feedback amplifier.

In addition to symbolic forms of transfer functions, we can also express time-domain responses in a semi-symbolic form. Idealized circuit models often used in the symbolic analysis lead to responses with multiple poles and zeros, which decreases the accuracy of standard algorithms. Paper [5.21] overcomes this problem by the use of a method for the accurate Jordan decomposition of matrix.

Developed methods for the symbolic analysis have been implemented in our symbolic simulator SNAP, which is utilized both in academia and industry worldwide [5.22].

The efficiency of the method can be demonstrated by the reduction of complexity of the transfer function of a circuit with a current-feedback amplifier, see Fig. 5.2.

The maximum allowed error of  $\pm 1.5$  dB and  $\pm 3^\circ$  was checked on two reference frequencies 1 kHz and 600 kHz. The first parametric step reduced the original 100 network parameters to 14. The topology transformation further decreased the number of symbolic terms to 4 in the numerator and to 65 in the denominator. The duration of the analysis was 7.1 s, see Tab. 5.1.

In the field of methods for testing analog circuits, the research was focused on the multi-frequency parametric

fault diagnosis [5.23]. The diagnosis is aimed at estimating the actual values of some network parameters from frequency-domain measurements of circuit characteristics. Circuit components, whose parameters exceed the allowed tolerance intervals, are classified as faulty.

		<i>parametric</i>	<i>topology</i>	<i>formula</i>
$\Delta M_{\max}$	allowed	$\pm 1.5\text{dB @ 1kHz and 600kHz}$		
	real	0.47dB @1kHz	0.56dB @600kHz	0.21dB @1kHz
$\Delta\varphi_{\max}$	allowed	$\pm 3^\circ @ 1\text{kHz and } 600\text{kHz}$		
	real	2.4° @600kHz	2.4° @600kHz	3.0° @600kHz
$k_N$		44	4	3
$k_D$		232	65	46
$n_p$		14	14	14
<i>runtime</i>		4.9s	1.3s	0.9s

Tab. 5.1. Results of simplification steps for CFA ( $\Delta M_{\max}$  is magnitude error,  $\Delta\varphi_{\max}$  – phase error,  $k_N$ ,  $k_D$  – the number of symbolic terms in the numerator and the denominator,  $n_p$  – the number of circuit parameters).

An optimal method for test frequency selection has not been determined yet. A measure introduced in [5.23], which maximizes sensitivities of network parameters in the frequency domain and minimizes the conditionality of the Jacobian matrix, seems to be a good measure for the test set optimality evaluation. An optimum set of test frequencies can be determined by minimizing the measure using a global stochastic optimization technique. Our solution is based on a modified Particle Swarm Optimization [5.24]. The method excels in the high convergence rate, no discretization of the solution and very easy implementation.

With respect to frequency set mirroring and the approach of agent reduction, the final phase of the optimization can be greatly accelerated. The error for the parameter estimation process is evaluated at a low number of test frequencies only.

In order to improve the result accuracy, a method based on an over determined system of fault equations was developed [5.24]. Conventional methods for the test frequency selection do not take into account manufacturing tolerances of real circuit components and measurement errors. For this reason, a robust method based on the Monte-Carlo tolerance analysis, which can overcome those problems, was proposed [5.25].

Furthermore, in the case of a band-pass filter test frequency selection, a simple heuristic solution can be used. In accordance with [5.26], individual test frequencies should be distributed symmetrically around the center frequency of the filter.

The complexity of generated symbolic formulae grows exponentially with the number of circuit components. Therefore, the fault diagnosis of large-scale circuits may be very difficult and computationally expensive. For this reason, a method based on the parametric reduction of the Jacobian matrix [5.27] or an approximate parametric fault diagnosis [5.28] can be used to reduce the computational complexity. Both methods involve a frequency-se-

lective identification of individual network parameters. The parameters that have weak effect on circuit frequency characteristics can be omitted. The methods are also applicable for the parasitic parameter estimation of real circuits [5.29].

The method for the test frequency selection, which is based on PSO, is demonstrated on a simple example of the frequency filter shown in Fig. 5.3. For nominal values of components  $R_1 = R_2 = R = 159.1 \Omega$ ,  $C_1 = C_2 = C = 1 \text{ nF}$  and  $g_m = 18.23 \text{ mS}$ , the filter is tuned to the center frequency  $f_c = 1 \text{ MHz}$  with the quality factor  $Q = 10$ .

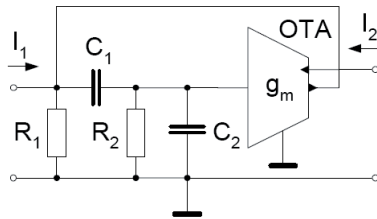


Fig. 5.3. Tunable 2<sup>nd</sup> order band-pass filter in current-mode.

One test point, which corresponds to  $I_2$ , and a testable group ( $R_2, g_m$ ) are considered. For robust fault diagnosis, at least two test frequencies have to be determined. The fault diagnosis represents a 2-dimensional optimization problem. The shape of the fitness function is shown in Fig. 5.4.

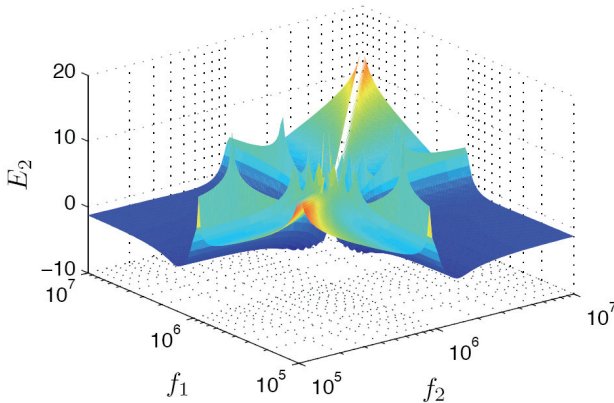


Fig. 5.4. Shape of fitness function for testable group ( $R_2, g_m$ ).

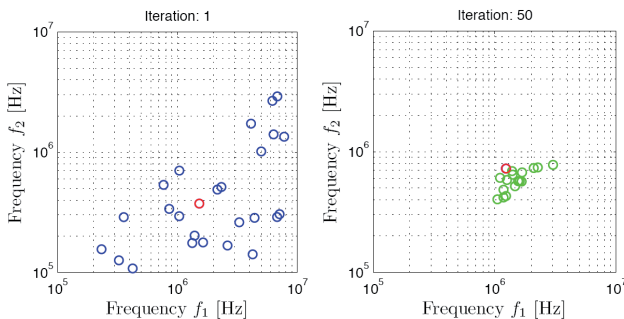


Fig. 5.5. Agent positions in searched space of optimization coordinates.

The position of each agent during the optimization is shown in Fig. 5.5. The inactive agents are represented by the green points. The red point corresponds to the global optimum found so far, i.e. the optimal set of test frequen-

cies. The original contribution of our research was published in [5.18] to [5.22] and [5.24] to [5.29]. Results can be exploited in the design and testing of analog and digital circuits in discrete or integrated technology.

## 6. Advanced Signal Processing

Signal processing techniques are essential for proper operation of advanced communication systems. Since the topic is extremely extensive, we decided to concentrate on three items only, on dirty RF signal processing, optimization of multi-carrier systems, and spectrum sensing.

### 6.1 Dirty-RF Signal Processing

We can increase the performance of communication systems by using modulations with a non-constant envelope and a wide bandwidth. Without any modification of the transmitter architecture, the use of a power amplifier (PA) operating far from the saturation point became inevitable.

On the contrary, the operating point of a PA is requested to be set close to the saturation point to achieve the maximal power efficiency (battery life). In such a region, the nonlinear effects are very strong. The nonlinearities in a PA generate amplitude and phase distortions causing spectral spreading in adjacent channels, inter-symbol interference or deformations of constellation diagrams [6.1].

As a result of the wide bandwidth of transmitted signals (i.e. from 20 MHz up to 100 MHz for the LTE system), memory effects of PAs are accentuated. Thus, PA linearization methods have to be used. PA linearization together with IQ imbalance compensation belong to the so-called “dirty-RF signal processing” methods.

There are several techniques to remove unwanted distortions such as digital predistortion (PD) [6.2]. A predistorter is a functional block that precedes a nonlinear device such as a PA. The signal of the input passes through the predistorter implemented often as the digital signal processing block whose characteristic is an inverse of the PA. The comparison of spectra (input data signal, PA output without predistortion, PA output with predistortion) for the wideband OFDM signal in the PD system is shown in Fig. 6.1.

For PD adaptation, either the direct or the indirect learning architecture can be used [6.3]. The indirect learning architecture solution [6.2] involves the use of a post-distorter for modeling a PA (as an inverse function to the predistorter), and then using the estimated coefficients for a predistorter implemented using either look-up tables [6.4], Volterra series or its derivatives (polynomials, orthogonal polynomials ...).

Our current activities in this domain mainly include the implementation of a digital predistorter for multi-standard applications, and researching the influence of

imperfections of RF components on the wideband PD performance.

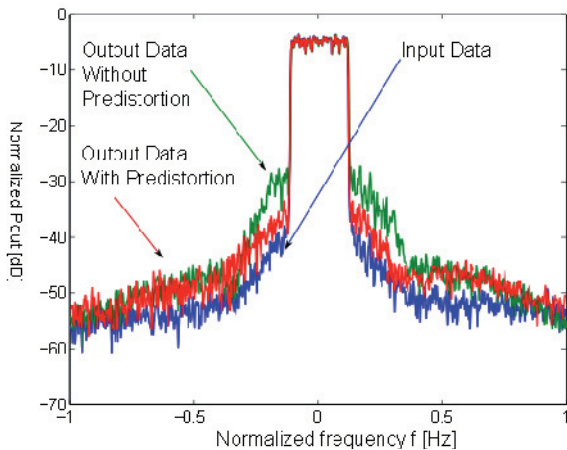


Fig. 6.1. Power spectral density of the input signal (blue), PA output without PD (green), and PA output with PD (red).

### 6.2 Multicarrier System Optimization

Many current and future communication systems are based on multi-carrier modulations (MCM) like OFDM (Orthogonal Frequency Division Multiplex). LTE (Long Term Evolution) and WiMAX are examples of OFDM-based systems.

The use of OFDM improves the performance in fading channel environments and makes channel equalization easier. In order to optimize the performance with respect to channel conditions, the adaptive OFDM was proposed in the past.

Various methods of OFDM optimization were developed. We can usually optimize the modulation order and the power at individual OFDM subcarriers. Most of the methods belong to so-called water-filling family [6.5].

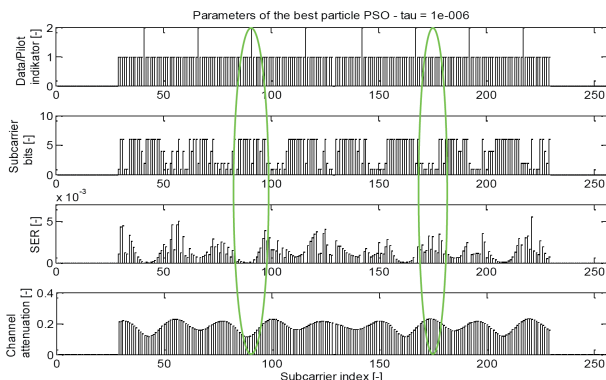


Fig. 6.2. OFDM optimization example.

In [6.6] and [6.7], we investigated the application of OFDM optimization methods in WiMAX and MB-OFDM standards. We tested and compared two approaches, the greedy optimization and the particle swarm optimization

(PSO). We evaluated the results using MATLAB simulations, and concluded that the performance of both methods is comparable. The illustrative example of the application to a fixed WiMAX system is shown in Fig. 6.2.

In order to make the adaptation possible, the periodic channel estimation or the symbol error rate computation has to be performed. In [6.8], we tried to reduce the adaptation complexity using an error-vector-magnitude parameter.

### 6.3 Spectrum Sensing

The dynamic spectrum access (DSA) in connection with the cognitive radio is a promising technique for future communication systems and networks. Spectrum sensing is one of the key components of DSA. The problem of spectrum sensing is equivalent to the classical hypothesis testing problem with the hypothesis  $H_1$  representing the presence of the primary user signal and the hypothesis  $H_0$  corresponding to its absence (presence of only noise).

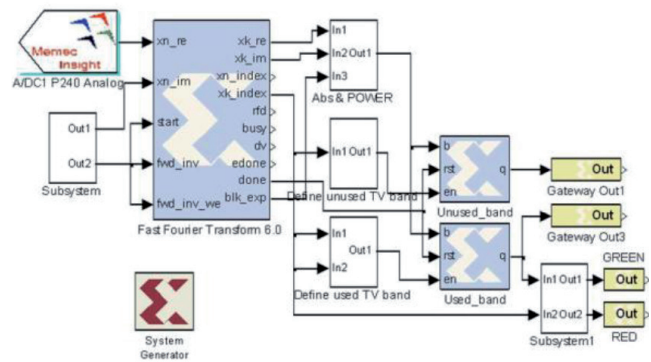


Fig. 6.3 Simplified implementation of a FPGA-based energy detector.

Several spectrum sensing methods (e.g. energy detection, correlation detection, eigenvalue based detection or cyclo-stationarity detection) have been proposed. Some of them were also included into standards like IEEE 802.22 for internet access in rural areas.

During our research, we started with basic energy-detector based spectrum sensing and its FPGA implementation in a Xilinx System Generator [6.9] (see the block schematics shown in Fig. 6.3). We continued with more advanced methods as goodness-of-fit statistical test methods (e.g., the Kolmogorov-Smirnov method).

Subsequently, we proposed a way of using information from the sensing process in the OFDM optimization algorithm in order to limit the interferences to primary users [6.10].

The original contribution of our research was published in [6.1] and [6.6] to [6.10]. Knowledge obtained can be exploited in software defined adaptive radio systems and cognitive radio systems dominantly.

## 7. Summary

The design of advanced communication systems is a multidisciplinary task:

1. The communication system has to be designed in its whole. Requirements on the functionality of the system define parameters of its individual blocks. Properties of selected systems are described in Section 2.
2. The electromagnetic environment of the system is crucial for its operation. Therefore, communication channels of systems have to be carefully modeled considering specific features of the environment. Selected channel models are described in Section 3.
3. Importance of antenna results in their ability to perform filtering both in the frequency domain and in the spatial domain. Filtering abilities of antennas can be exploited when synthesizing a required frequency response of an antenna in the direction of communication as described in Section 4.
4. Communication signals are further processed by electronic circuits and signal processing techniques. Electronic circuits take care of filtering and amplifying signals as described in Section 5. Signal processing techniques are applied to suppress distortions, to exploit multi-carrier transmissions and to sense information about frequency spectrum properties. Detailed information is given in Section 6.

The corresponding research was performed by the consortium of the COST Action IC0803 RF/Microwave Communication Subsystems for Emerging Wireless Technologies. Research activities of Brno University of Technology within this COST were supported by the grant OC09016 Components and Advanced Radio Communication Systems provided by the Czech Ministry of Education.

## Acknowledgements

Research described in this paper was financially supported by the grant OC09016 provided by the Czech Ministry of Education.

The support of the project CZ.1.07/2.3.00/20.0007 WICOMT, financed from the operational program Education for Competitiveness, is gratefully acknowledged.

The described research was performed in laboratories supported by the SIX project; the registration number CZ.1.05/2.1.00/03.0072, the operational program Research and Development for Innovation.

## References

- [1.1] DANIELS, R.C., HEATH, R.W. 60 GHz wireless communications: emerging requirements and design recommendations. *IEEE Vehicular Technology Magazine*, 2007, vol. 2, no. 3, p. 41–50.
- [1.2] STALLO, C., MUKHERJEE, S., CIANCA, E., ROSSI, T., DE SANCTIS, M., RUGGIERI, M. Performance analysis of an IR-UWB transceiver architecture for multi-gigabit/s LOS links in W band. In *Proceedings of the 2010 IEEE International Conference on Ultra-Wideband*. Nanjing (China): IEEE, 2010.
- [1.3] PITRA, K., RAID, Z., BARTYZAL, J. Antenna structures for emerging frequency bands. In *Proceedings of the 18<sup>th</sup> Telecommunications Forum TELFOR 2010*. Belgrade (Serbia): IEEE, 2010. ISBN: 978-86-7466-392-9.
- [1.4] FETTE, B. A. *Cognitive Radio Technology*. Second Edition. Burlington: Elsevier, 2009. ISBN 978-0-12-374535-4.
- [1.5] ZHANG, D., SHINKUMA, R., MANDAYAM, N. B. Bandwidth exchange: an energy conserving incentive mechanism for cooperation. *IEEE Transactions on Wireless Communication*, 2010, vol. 9, no. 6, p. 2055-2065.
- [1.6] VALENTA, V., BAUDOIN, G., VILLEGAS, M., MARŠÁLEK, R. Hybrid dual-mode frequency synthesis for cognitive multi-radio front-ends. *Wireless Personal Communications*, 2012, vol. 64, no. 1, p. 197-210. ISSN: 0929-6212.
- [2.1] HAYKIN, S. Cognitive radio: brain-empowered wireless communications. *IEEE Journal on Selected Areas in Communications*, 2005, vol. 23, no. 2, p. 201-220.
- [2.2] IEEE Computer Society, IEEE Standard for Information Technology—Telecommunications and information Exchange between systems Wireless Regional Area Networks (WRAN)—Specific requirements, Part 22: Cognitive Wireless RAN Medium Access Control (MAC) and Physical Layer (PHY) Specifications: Policies and Procedures for Operation in the TV Bands, IEEE Std. 802.22-2011, 1 July 2011.
- [2.3] VALENTA, V., MARSALEK, R., BAUDOIN, G., VILLEGAS, M., SUAREZ PENALOZA, M., ROBERT, F. Survey on spectrum utilization in Europe: measurements, analyses and observations. In *Proceedings of the 5th International Conference on Cognitive Radio Oriented Wireless Networks and Communications*. Cannes (France): IEEE, 2010. p. 101-105.
- [2.4] ALAGHA, S., KABAL, P. Generalized raised cosine filters. *IEEE Transactions on Communication*, 1999, vol. 47, no.7, p. 989-997.
- [2.5] FARHANG-BOROUJENY, B. Nyquist filters with robust performance against jitter. *IEEE Transactions on Signal Processing*, 1998, vol. 46, no. 12, p. 3427-3431.
- [2.6] BOONYANANT, P., TANTARATANA, S. Design and hybrid realization of FIR Nyquist filters with quantized coefficients and low sensitivity to timing jitter. *IEEE Transactions on Signal Processing*, 2005, vol. 53, no. 1, p. 208-221.
- [2.7] ZHANG, X., YOSHIKAWA, T. Design of FIR Nyquist filters with low group delay. *IEEE Transactions on Signal Processing*, 1999, vol. 47, no. 5, p. 1454-1458.
- [2.8] HERMES, D., KRAGH, F. A bandwidth efficient constant envelope modulation. In *Proceedings of Fortieth Asilomar Conference on Signals, Systems and Computers ACSSC 2006*. Pacific Grove (California): IEEE, 2006, p. 488-492.
- [2.9] CHATELAIN, B., GAGNON, F. Peak-to-average power ratio and inter-symbol interference reduction by Nyquist pulse optimization. In *Proceedings of the Vehicular Technology Conference VTC 2004*. IEEE, 2004, p. 954-958.
- [2.10] HARRIS, J. F. On the use of windows for harmonic analysis with the discrete Fourier transform. *Proceedings of the IEEE*, 1978, vol. 66, no. 1, p. 51-83.
- [2.11] BEAULIEU, C. N., et al., A “better than” Nyquist pulse. *IEEE Communications Letters*, 2001, vol. 5, no.9, p. 367-368.
- [2.12] BOBULA, M., PROKES, A., DANEK, K. Nyquist filters with alternative balance between time and frequency-domain parameters. *EURASIP Journal on Advances in Signal Processing*, 2010,

- vol. 2010, p./rec. no: 903980.
- [2.13] SAYED, A. H., TARIGHAT, A., KHAJEHNOURI, N. Network based wireless location: challenges faced in developing techniques for accurate wireless location information. *IEEE Signal Processing Magazine*, 2005, vol. 22, no. 4, p. 24-40.
- [2.14] ZHANG, Y., LI, X., AMIN, M. G. *RFID Systems: Research Trends and Challenges. Principles and Techniques of RFID Positioning*. Chichester: John Wiley & Sons, 2010, p. 389-415.
- [2.15] LI, X., ZHANG, Y., AMIN, M. G. Multi-frequency-based range estimation of RFID tags. In *Proceedings of the IEEE Internat. Conference on RFID 2009*. Orlando (USA), 2009, p. 147-154.
- [2.16] POVALAC, A., SEBESTA, J. Phase difference of arrival distance estimation for RFID tags in frequency domain. In *Proceedings of the 2011 IEEE International Conference on RFID-Technologies and Applications*. Barcelona (Spain), 2011, p. 180-185.
- [3.1] RAPPAPORT, T. S. *Wireless Communications: Principle and Practice*. 2<sup>nd</sup> ed. USA: Prentice Hall, 2002.
- [3.2] KLOZAR, L., PROKOPEC, J. Propagation path loss models for mobile communication. In *Proceedings of the 21<sup>st</sup> International Conference Radioelektronika 2011*, Brno (Czechia): Brno University of Technology, 2011, p. 287-290.
- [3.3] KLOZAR, L., PROKOPEC, J., HANUS, S., SLANINA, M., FEDRA, Z. Indoor channel modeling based on outdoor urban measurement: multi-slope modeling. In *Proc. of the IEEE International Conf. on Microwaves, Communications, Antennas and Electronic Systems COMCAS 2011*. Tel Aviv (Israel): IEEE, 2011.
- [4.1] CHENG, D. K. Gain optimization for Yagi-Uda arrays. *IEEE Antennas and Propagation Magazine*, 1991, vol. 33, no. 3, p. 42 to 45.
- [4.2] JONES, E. A., JOINES, W. T. Design of Yagi-Uda antennas using genetic algorithms. *IEEE Transactions on Antennas and Propagation*, 1997, vol. 45, no. 9, p. 1386-1392.
- [4.3] VENKATARAYALU, N. V., RAY, T. Optimum design of Yagi-Uda antennas using computational intelligence. *IEEE Transact. on Antennas and Propagation*, 2004, vol. 52, no. 7, p. 1811 to 1818.
- [4.4] DEB, K. *Multi-Objective Optimization using Evolutionary Algorithms*. Chichester, UK: J. Wiley and Sons, 2001.
- [4.5] KADLEC, P., RAIDA, Z. A novel multi-objective self-organizing migrating algorithm. *Radioengineering*, 2011, vol. 20, no. 4, p. 77 to 90.
- [4.6] KADLEC, P., RAIDA, Z. Self-organizing migrating algorithm for optimization with general number of objectives. In *Proceedings of 22nd International Conference Radioelektronika*, 2012, Brno: Brno University of Technology, p. 111-115.
- [5.1] BIOLEK, D., SENANI, R., BIOLKOVA, V., KOLKA, Z. Active elements for analog signal processing: classification, review and new proposals. *Radioengineering*, 2008, vol. 17, no. 4, p. 15-32.
- [5.2] SOTNER, R., PETRZELA, J., SLEZAK, J. Current-controlled current-mode universal biquad employing multi-output transconductors. *Radioengineering*, 2009, vol. 18, no. 3, p. 285-294.
- [5.3] SOTNER, R., JERABEK, J., HERENC SAR, N., DOSTAL, T., VRBA, K. Additional approach to the conception of current follower and amplifier with controllable features. In *Proc. of the 34th International Conference on Telecommunications and Signal Processing TSP 2011*, Budapest (Hungary), p. 279-283.
- [5.4] SOTNER, R., SLEZAK, J., DOSTAL, T. Influence of mirroring of current output responses through grounded passive elements. In *Proc. of the 20th International Conference Radioelektronika 2010*. Brno (Czech Republic), p. 177-180.
- [5.5] JERABEK, J., SOTNER, R., VRBA, K. Tunable universal filter with current follower and transconductance amplifiers and study of parasitic influences. *Journal of Electrical Engineering*, 2011, vol. 62, no. 6, p. 317-326.
- [5.6] PETRZELA, J., DRINOVSKY, J. High frequency chaos converters. In *Proc. of the International Conference on Computational Technologies in Electrical and Electronics Engineering SIBIR-CON 2010*. Irkutsk (Russia), p. 750-754.
- [5.7] SOTNER, R., JERABEK, J., PETRZELA, J., DOSTAL, T., VRBA, K. Electronically tunable simple oscillator based on single-output and multiple-output transconductor. *IEICE Electronics Express*, 2009, vol. 6, no. 20, p. 1476-1482.
- [5.8] SOTNER, R., HRUBOS, Z., SLEZAK, J., DOSTAL, T. Simply adjustable sinusoidal oscillator based on negative three-port current conveyors. *Radioengineering*, 2010, vol. 19, no. 3, p. 446-453.
- [5.9] SOTNER, R., JERABEK, J., PROKOP, R., VRBA, K. Current gain controlled CCTA and its application in quadrature oscillator and direct frequency modulator. *Radioengineering*, 2011, vol. 20, no. 1, p. 317-326.
- [5.10] SOTNER, R., HRUBOS, Z., SEVCIK, B., SLEZAK, J., PETRZELA, J., DOSTAL, T. An example of easy synthesis of active filter and oscillator using signal flow graph modification and controllable current conveyors. *Journal of Electrical Engineering*, 2011, vol. 62, no. 5, p. 258-266.
- [5.11] SOTNER, R., JERABEK, J., HERENC SAR, N., HRUBOS, Z., DOSTAL, T., VRBA, K. Study of adjustable gains for control of oscillation frequency and oscillation condition in 3R-2C oscillators. *Radioengineering*. 2012, vol. 21, no. 1, p. 392-402.
- [5.12] PETRZELA, J., VYSKOCIL, P., PROKOPEC, J. Fundamental oscillators based on diamond transistors. In *Proc. of the 20th International Conference Radioelektronika 2010*. Brno (Czech Republic), p. 217-220.
- [5.13] CHANG, H., KUNDERT, K., Verification of complex analog and RF IC designs. *Proceedings of the IEEE*, 2007, vol. 95, no. 3, p. 622-639.
- [5.14] SOMMER, R., HALFMANN, T., BROZ, J. Automated behavioral modeling and analytical model-order reduction by application of symbolic circuit analysis for multi-physical systems. *Simulation Modelling Practice and Theory*, 2008, no. 16, p. 1024-1039.
- [5.15] DAEMS, W., GIELEN, G., SANSEN, W. Circuit simplification for the symbolic analysis of analog integrated circuits. *IEEE Transactions on Computer Aided Design*, 2002, vol. 21, no. 4, p. 395-407.
- [5.16] HENNIG, E. *Symbolic Approximation and Modeling Techniques for Analysis and Design of Analog Circuits*. Ph.D. dissertation, University of Kaiserslautern (Germany), 2000.
- [5.17] YU, Q., SECHEN, C. A unified approach to the approximate symbolic analysis of large analog integrated circuits. *IEEE Transactions on Circuits and Systems I*, 1996, vol. 43, no. 8, p. 656-69.
- [5.18] KOLKA, Z., BIOLEK, D., BIOLKOVA, V., HORAK, M. Implementation of topological circuit reduction. In *Proceedings of the 11th Biennial IEEE Asia Pacific Conference on Circuits and Systems (APCCAS 2010)*. Malaysia: IEEE, 2010, p. 951-954.
- [5.19] KOLKA, Z., VLK, M., HORAK, M. Topology reduction for approximate symbolic analysis. *Radioengineering*, 2011, vol. 20, no. 1, p. 252-256.
- [5.20] KOLKA, Z., BIOLEK, D., BIOLKOVA, V., DOBEŠ, J. Tolerance-based control mechanism for approximate symbolic analysis. In *Proc. of the IEEE Africon 2011 Conf.*. Zambia: IEEE, 2011, p. 1-5.
- [5.21] KOLKA, Z., BIOLEK, D., BIOLKOVA, V. Accurate time-domain semi symbolic analysis. In *Proc. of 11th International Workshop on Symbolic and Numerical Methods, Modeling and Application to Circuit Design SM2ACD 2010*. Tunis: IEEE, 2010, p. 137-140.

- [5.22] KOLKA, Z.; BIOLEK, D.; KALOUS, J.; BIOLKOVA, V. Program for Multi-Domain Symbolic Analysis. In *Proceedings of XIth International Workshop on Symbolic and Numerical Methods, Modeling and Application to Circuit Design SM2ACD 2010*. Tunisia: IEEE, 2010. p. 120-123.
- [5.23] GRASSO, F., LUCHETTA, A., MANETTI, S., PICCIRILLI, M.C. A method for the automatic selection of test frequencies in analog fault diagnosis. *IEEE Transactions on Instrumentation and Measurement*, 2007, vol. 56, no. 6, p. 2322-2329.
- [5.24] KINCL, Z., KOLKA, Z. Parametric fault diagnosis using over determined system of fault equations. In *Proceedings of the 3rd International IEEE Conference on Microwaves, Communications, Antennas and Electronic Systems COMCAS 2011*. Tel-Aviv (Israel), 2011, p. 1-4.
- [5.25] KINCL, Z., KOLKA, Z., SOTNER, R. Simple method for test frequency selection using tolerance analysis. In *Proceedings of the 18th International Conference Mixed Design of Integrated Circuits and Systems 2011*. Gliwice (Poland), 2011, p. 511-515.
- [5.26] KINCL, Z., KOLKA, Z. Test frequency selection for band-pass filters. In *Proceedings of the 20<sup>th</sup> International Conference Radioelektronika 2010*. Brno (Czech Republic), 2010, p. 173-176.
- [5.27] KOLKA, Z., KINCL, Z., BIOLEK, D., BIOLKOVÁ, V. Parametric reduction of Jacobian matrix for fault analysis. In *Proc. of the 22nd IEEE International Conference on Microelectronics (ICM 2010)*. Cairo: IEEE, 2010. p. 503-506.
- [5.28] KINCL, Z., KOLKA, Z. Approximate parametric fault diagnosis. In *Proc. of the 21st International Conference Radioelektronika 2011*. Brno: Brno University of Technology, 2011, p. 199-202.
- [5.29] KINCL, Z., KOLKA, Z., BIOLKOVA, V. Parasitic parameter estimation using multi-frequency parametric fault diagnosis. In *Proc. of the 22nd International Conference Radioelektronika 2012*. Brno: Brno University of Technology, 2012.
- [6.1] DVORAK, J., MARSALEK, R. Simulation of multi-carrier and single-carrier transmission mode for millimeter-wave high speed transmission in presence of transmitter imperfections. In *Proceedings of 34th International Conference on Telecommunications and Signal Processing, TSP 2011*. 2011. p. 91-94.
- [6.2] MARSALEK, R., JARDIN, P., BAUDOIN, G. From post distortion to predistortion for power amplifiers linearization. *IEEE Communications Letters*, 2003, vol. 7, no. 7.
- [6.3] PAASO, H., MAMMELA, A. Comparison of direct learning and indirect learning predistortion architectures. In *Proceedings of Wireless Communication Systems ISWCS 2008*, Reykjavik: IEEE, 2008.
- [6.4] JARDIN, P., BAUDOIN, G. Filter look up table method for power amplifier linearization. *IEEE Transactions on Vehicular Technology*, 2007, vol. 56, no. 3.
- [6.5] PAPANDREOU, N., ANTONAKOPOULOS, T. Bit and power allocation in constrained multicarrier systems: the single-user case. *EURASIP Journal on Advances in Signal Processing*, 2008, vol. 2008.
- [6.6] AL-SHERBAZ, A., KUSELER, T., ADAMS, C., MARSALEK, R., POVALAC, K. WiMAX parameters adaptation through a baseband processor using discrete particle swarm method. *International Journal of Microwave and Wireless Technologies*, 2010, vol. 2010, no. 2, p. 165-171.
- [6.7] POVALAC, K., MARSALEK, R. Adaptation of multicarrier based UWB system parameters using swarm optimization. In *Proceedings of the 4th IEEE UWB Forum on Sensing and Communications*. TU Vienna (Austria), 2009.
- [6.8] MARSALEK, R., POVALAC, K., DVORAK, J. Use of the error vector magnitude for low-complex bit loading in orthogonal frequency division multiplexing. In *Proceedings of the 7th International Symposium on Image and Signal Processing and Analysis*. 2011. p. 42-45.
- [6.9] POVALAC, K., MARSALEK, R., BAUDOIN, G., SRAMEK, P. Real-time implementation of periodogram based spectrum sensing detector in TV bands. In *Proceedings of 20th International Conference Radioelektronika 2010*. Brno: Brno University of Technology, p. 137-140.
- [6.10] POVALAC, K., MARSALEK, R., SRAMEK, P. Optimization of multicarrier communication system with respect to imperfect sensing. In *Proceedings of 33rd International Conference TSP 2010*. Baden near Vienna (Austria), 2010.